
Article:
Best, A., Ashby, B., White, A. et al. (4 more authors) (2017) Host-parasite fluctuating selection in the absence of specificity. Proceedings of the Royal Society B: Biological Sciences, 284 (1866). 20171615. ISSN 0962-8452

https://doi.org/10.1098/rspb.2017.1615

Host-parasite fluctuating selection in the absence of specificity

Alex Best[1*], Ben Ashby[2,3], Andy White[4], Roger Bowers[5], Angus Buckling[6], Britt Koskella[3] and Mike Boots[3,6]

[1]*School of Mathematics & Statistics, University of Sheffield, Sheffield, S3 7RH, UK.*

[2]*Department of Mathematical Sciences, University of Bath, Claverton Down, Bath, BA2 7AY, UK.*

[3]*Department of Integrative Biology, University of California Berkeley, Berkeley, CA, USA.*

[4]*Department of Mathematics and the Maxwell Institute for Mathematical Sciences, Heriot-Watt University, Edinburgh, EH14 4AS, Scotland, UK.*

[5]*Department of Mathematical Sciences, Division of Applied Mathematics, Mathematical Sciences Building, The University of Liverpool, L69 7ZL, UK.*

[6]*Biosciences, College of Life and Environmental Sciences, University of Exeter, Cornwall Campus, Treliever Road, Penryn, Cornwall, TR10 9EZ, UK.*

** Corresponding author*

Running Head: Cycles in host-parasite coevolution

Abstract

Fluctuating selection driven by coevolution between hosts and parasites is important for the generation of host and parasite diversity across space and time. Theory has focused primarily on infection genetics, with highly specific 'matching allele' frameworks more likely to generate fluctuating selection dynamics (FSD) than 'gene-for-gene' (generalist-specialist) frameworks. However, the environment, ecological feedbacks, and life-history characteristics may all play a role in determining when FSD occurs. Here, we develop eco-evolutionary models with explicit ecological dynamics to explore the ecological, epidemiological and host life-history drivers of FSD. Our key result is to demonstrate for the first time that specificity between hosts and parasites is not required to generate FSD. Furthermore, highly specific host-parasite interactions produce unstable, less robust stochastic fluctuations in contrast to interactions that lack specificity altogether or those that vary from generalist to specialist, which produce predictable limit cycles. Given the ubiquity of ecological feedbacks and the variation in the nature of specificity in host parasite interactions, our work emphasizes the underestimated potential for host-parasite coevolution to generate fluctuating selection.

Key Words

Coevolution, infectious disease, fluctuating selection, specificity

Introduction

Understanding the coevolution of hosts and parasites is important given the central role that infectious disease plays in human health, agriculture and natural systems. Theory predicts that the coevolution of hosts and their parasites may lead to a number of distinct outcomes, including a co-evolutionary stable strategy (co-ESS) for both host and parasite [1,2]; static within population dimorphism or polymorphism [2-5]; escalation (known as arms race dynamics, ARD) [6]; and fluctuating selection dynamics (FSD) [7-11]. Arms race dynamics cannot continue indefinitely due to associated fitness costs or physiological constraints (e.g. [12]), which means that, in the long term, coevolution will eventually lead to either a stable evolutionary equilibrium (including polymorphisms) or fluctuating selection. Fluctuating selection is therefore of particular importance because it is the only dynamic coevolutionary outcome that can be maintained indefinitely in a constant environment. The presence of a constantly changing antagonist is thought to play a key role in the maintenance of diversity [13], and also has implications for selection for sex and recombination [14-16], and local adaptation [17-19]. Understanding the processes and mechanisms that promote FSD therefore has significant implications for our understanding of a wide range of biological phenomena.

Theoretical work has primarily focused on how different forms of genetic specificity between hosts and parasites lead to fluctuating selection [7-11;19-21]. Highly specific 'matching allele' interactions, where parasites must 'match' the host at each loci to infect, commonly generate coevolutionary 'cycles' (i.e. FSD) as

selection favors parasite genotypes capable of infecting common host genotypes, thereby generating negative frequency-dependent selection [20-22]. Effectively, hosts constantly evolve to 'escape' parasites that can infect them while parasites play 'catch-up'. In contrast, 'gene-for-gene' interactions (where there is variation in specificity such that hosts and parasites vary from specialists to generalists) often produce arms race dynamics (ARD), where directional selection favors increasing resistance and infectivity ranges, although there can be a transition to FSD if there are costs to infection and defense [7-11]. While some empirical evidence appears consistent with the notion that different genetic interactions are associated with ARD or FSD [23-25], recent experimental work has shown that changing environmental conditions can cause host-parasite interactions to switch between ARD and FSD [26-28], suggesting either that the environment determines specificity or that the same genetic specificity has different consequences depending on the environment.

One way to investigate the importance of genetic specificity alongside ecological feedbacks in determining FSD is to directly compare coevolutionary dynamics with no specificity with those generated under various different forms of specificity. This can be achieved using eco-evolutionary models, which allow for varying population sizes due to changes in host defence and parasite infectivity. These models are increasingly used to examine the role of environmental and ecological feedbacks on the coevolution of hosts and parasites [1,2,4,5,29] and have largely considered the processes that determine co-ESS levels of host defense and parasite infectivity, and the potential for diversification through evolutionary branching. For example, it has been shown that the likelihood of

95 static, within-population diversification depends on the nature of host-parasite
96 genetic specificity, associated fitness costs, and explicit ecological dynamics [5].
97 The form of the infection interaction was crucial to the level of diversity that
98 could arise, with non-specific 'universal' functions (parasite A always has higher
99 transmission than parasite B against any host) leading to dimorphism at most,
100 but 'range' functions with variation in specificity (whereby the relative success of
101 parasite strains depends on the target host) potentially leading to higher levels
102 of polymorphism [5]. This work emphasized the important role that ecological
103 feedbacks play in host-parasite coevolution. Little of this work, however, has
104 considered the potential for fluctuating selection [4,27] and none has provided a
105 full exploration of the ecological, epidemiological and host life-history drivers of
106 FSD.
107
108 Here we examine how host and parasite life-history characteristics and the
109 specificity of their interaction, in combination with ecological feedbacks,
110 determine the likelihood of fluctuating selection. By 'specificity', we mean the
111 degree to which parasite strains specialise on a subset of host types. An
112 interaction is defined to be 'specific' if each parasite strain has higher
113 transmission against some hosts and lower transmission against others
114 compared to another parasite strain. Conversely, an interaction is 'non-specific' if
115 each parasite strain always has either higher or lower transmission against all
116 hosts compared to another parasite strain. We consider interactions between
117 hosts and parasites starting from 'universal' (all non-specific), to 'range'
118 (variation from highly specific to generalist, and therefore phenotypically
119 equivalent to gene-for-gene models but with continuous phenotypic variation),

and 'matching' (highly specific, where all parasite strains are specialists on respective host strains, and therefore phenotypically equivalent to matching allele models but again with continuous phenotypic variation). Furthermore we explicitly consider the ecological and epidemiological settings that promote cycles. As such we determine what factors and which types of host-parasite interactions promote fluctuating selection.

Model and Methods

We base our mathematical analysis within the eco-evolutionary invasion framework known as adaptive dynamics [30-33] and combine this with explicit evolutionary simulations that relax some of the restrictive assumptions of the mathematical approach (see §A1 in SI for a fuller description of the analytic methods, and §B for a description of the numerical simulations). We assume that resident strains of host and parasite have reached a population dynamic equilibrium of a Susceptible – Infected – Susceptible model [5,34],

(1) $\frac{dS}{dt} = (a - q(S+I))(S + fI) - bS - \beta SI + \gamma I$

(2) $\frac{dI}{dt} = \beta SI - (b + \alpha + \gamma)I$.

Susceptible hosts reproduce at rate a, with the rate for infected hosts reduced by $f \in [0,1]$, with reproduction limited by competition by a density-dependent factor q. All hosts die at natural mortality rate b, but infected hosts suffer an additional mortality at rate , which we define as 'virulence' (in contrast to the plant-pathogen literature where virulence is often defined as infectivity).

145 Transmission is assumed to be a mass action density-dependent interaction with
146 coefficient β. We assume that both the host and parasite have some 'control'
147 over the transmission rate, so that transmission is dependent on the host trait, h,
148 and parasite trait p, with $\beta = \beta(h, p)$. We will generally define h as susceptibility
149 (I.e., inversely, resistance) and p as infectivity. Finally hosts can recover from
150 infection at rate γ. For our algebraic analysis we will make the simplifying
151 assumptions that $\gamma = 0$ and $f = 0$, but we shall relax these assumptions in our
152 numerical investigations.
153
154 We assume that a resident host (h) and parasite (p) are at their endemic steady
155 state and that a rare mutant strain of either the host ($\bar{h}$; overbars denoting
156 mutant traits) or parasite ($\bar{p}$) attempts to invade (with trait values limited to $h \in$
157 [0,1] and $p \in [0,1]$ by some physiological constraints). The mutant has small
158 phenotypic differences to the current resident strain and therefore a different
159 transmission coefficient. We assume trade-offs in which a decrease in
160 transmission (either an absolute reduction or an increase in resistance range;
161 see below) caused by a host mutation confers a cost to the host birth rate, $a(h)$,
162 while an increase in the base transmission rate caused by a parasite mutation
163 confers either an increase in virulence, $\alpha(p)$, or a reduced infection range [4,5].
164 The success of the mutant depends on its invasion fitness when the resident is at
165 its ecological equilibrium. In the simplified case where $\gamma = 0, f = 0$ (see SI §A1
166 for general case), the respective host and parasite fitnesses are,
167
168 (3) $s(\bar{h}; h, p) = a(\bar{h}) - q(\hat{S} + \hat{I}) - b - \beta(\bar{h}, p)\hat{I}$,
169 (4) $r(\bar{p}; h, p) = \beta(h, \bar{p})\hat{S} - b - \alpha(\bar{p})$

(where hats denote equilibrium densities of the resident). If a mutant has positive invasion fitness it will invade to replace or coexist with the current resident (subject to demographic stochasticity [30]), while if it has negative fitness it will die out. Through a series of mutations and substitutions the two species will coevolve in the directions of their local selection gradients, with the canonical equations [30,31] given by

$$\frac{dh}{dt} = \varphi^h \hat{S} \frac{\partial s}{\partial \bar{h}}\Big|_{\bar{h}=h} = \varphi^h \hat{S}[a_{\bar{h}} - \beta_{\bar{h}} \hat{I}] \quad (5)$$

$$\frac{dp}{dt} = \varphi^p \hat{I} \frac{\partial r}{\partial \bar{p}}\Big|_{\bar{p}=p} = \varphi^p \hat{I}[\beta_{\bar{p}} \hat{S} - \alpha_{\bar{p}}] \quad (6)$$

where subscripts denote derivatives (i.e. $\beta_{\bar{h}} = \partial\beta(\bar{h}, p)/\partial\bar{h}$) and φ^i controls the respective speeds of mutation (which are products of the mutation rate and variance and a factor of 1/2). To simplify what follows we shall set $\varphi^h = \varphi^p = 1$. Note that all the derivatives are evaluated at the resident trait values, $\bar{h} = h, \bar{p} = p$.

A coevolutionary 'singular point' is a point at which the two selection gradients are simultaneously zero (i.e. there is no longer directional selection on either species). There are four behaviors at a singular point that are of particular interest. First, the singular point can be a long-term attractor of evolution (*Continuously Stable Strategy* or CSS; a dynamic counterpart to the classic Evolutionarily Stable Strategy (ESS)). Second, the singular point can be an *evolutionary branching point* for that species. Here one of the species will

undergo disruptive selection and branch into two coexisting strains. Third, if varying parameter values causes the system to pass a critical point (a Hopf bifurcation [36]) then *coevolutionary cycles* will result (although further work is required to find whether the resulting cycles are stable, resulting in FSD, or unstable, resulting in bistability). Finally, a repelling singular point could cause directional selection in the host and/or parasite to *maximize or minimize* their investment to bounds of evolution (recall $h, p \in [0,1]$), while the other species may reach a purely evolutionary CSS (i.e. a host CSS may exist where *p=1*), may branch or may also maximize/minimize.

It is clearly important to examine the precise nature of the infection function, $\beta(h,p)$, to determine coevolutionary dynamics. Following previous work [5], here we use three key functional forms: 'universal' (no specificity), 'range' (variation from specialism to generalism), and 'matching' (highly specific). These are shown as heat maps in figure 1, where red denotes high transmission rates for combinations of *h* and *p* and blue low transmission. In detail:

The universal function is given by,

(7) $\beta(h,p) = \sigma(h)\rho(p) + k,$

where *k* is a constant giving the minimum value of the infection function. In this case there is no specificity, as figure 1a highlights that parasites retain the same relative ordering of infection rates against any host (see also fig S1a in the SI). As such, each host is 'universally' more resistant moving from right-to-left (here

$\beta_h > 0$, where the subscript denotes differentiation with respect to h) and similarly for parasites ($_p$ >0).

The range function is given by,

(8) $\beta(h,p) = \beta_0(p)\left(1 - \frac{1}{1+\exp(\kappa(p-h))}\right)$,

where κ is a constant controlling the steepness of the curve. In this case there is variation in specificity, representing hosts and parasites that range from specialist to generalist. A parasite trade-off, $\beta_0(p)$, is built in to the infection function so that parasites with a narrow range (low p) achieve higher transmission against the least resistant hosts (the cost of a large range is thus a low transmission rate, and we assume no further parasite trade-offs to virulence; including an additional virulence trade-off has no qualitative impact on the results presented here). The range function, as shown in figure 1b (see also fig S1b) therefore includes specificity as for low h parasites with low p have the highest transmission, but for high h parasites with high p are the most infectious. Hence, parasites vary in the range of hosts that they can successfully infect, and similarly for host resistance.

For the matching function,

(9) $\beta(h,p) = \beta_0(p)exp\left(-\left(\frac{p-h}{\eta p+c}\right)^2\right)$,

where η and c are constants controlling the variance of the infection curves. Here a 'match' between host and parasite strains is required for optimal infection, with the transmission rate falling away as they become more distant. This function therefore corresponds to a high degree of specificity between host and parasite. The case where η=0 and $\beta_0(p)$ is constant (i.e. there are no costs to the parasite) represents a continuous analogy of matching alleles infection genetics, as shown in figure 1c (see also fig S1c; e.g. [5]). When η>0 and we assume costs, the trade-off ensures that parasites with a narrow range achieve higher transmission against their matching hosts relative to parasites with a broader range (again, there is no virulence trade-off in the matching model), as shown in figure 1d (see also fig S1d). This is in some sense a hybrid matching-range function, but the maximum transmission of a parasite is not always against the least resistant hosts (compare figs 1b and 1d).

Results

Specificity of the infection function

In the SI §A2 we show that if there are no fitness costs to host resistance or parasite infectivity, then a coevolutionary singular point can never exist for the universal or range functions. Since selection now only acts on transmission the host will always evolve to minimize investment and the parasite to maximise (to bounds of evolution). For the matching function with no costs (i.e. figure 1c), there will be a continuum of singular points at $h=p$ none of which are attracting. Under the full assumptions of adaptive dynamics, this will lead to a random walk

through trait space. However, if we relax the assumption of mutations occurring rarely, fluctuating selection occurs due to the 'trail' of strains on one side of the current resident. This build up of strains keeps the host or parasite evolving in the same direction for longer, with reversals in selection due to one antagonist 'passing' the other becoming more rare. We term these '*stochastic oscillations*', since they are non-deterministic, unstable cycles whose existence depends on the discrete and stochastic assumptions of the simulations. An example of these stochastic oscillations can be found in [5]. For the remainder of this study we assume that host resistance and parasite infectivity are costly.

We initially consider whether coevolutionary cycles can ever emerge for each infection function. This is particularly important for the universal function since cycles in this model have never been demonstrated (see [4] and [27] for examples of cycles in the range model). To achieve this, initially we simply wish to show that parameters and trade-offs exist that produce a Hopf bifurcation, using a method previously employed to find cycles between parasite virulence and predator population densities [36]. The full analysis is given in the SI §A2.

In the universal model (7) cycles will be possible (for some parameters and trade-offs) wherever $k > 0$. However, there is a special case for $k=0$ (i.e. the minimum value of the infection function is 0), where we show there can never be cycles (see SI §A2i). Biologically, this means that cycles in quantitative levels of resistance and infectivity will not occur unless parasites have a non-zero baseline level of transmission, and is due to the host trait having no impact on parasite selection in this special case (see SI §A2i). This explains why in a

previous study we found no evidence of coevolutionary cycles with the universal transmission function $\beta(h,p) = hp$ [2]. Figure 2a shows numerical simulations of the coevolutionary dynamics for the case where $\beta(h,p) = hp + 0.5$ (i.e. $k > 0$) with regular coevolutionary cycles. These cycles lead to regular increases and decreases in quantitative host resistance and parasite infectivity (transmission) and virulence. The cycles arise simply due to the negative frequency dependence resulting from the epidemiological feedbacks on disease prevalence from the evolution of resistance and infectivity.

We find that a Hopf bifurcation may occur for any form of the range infection function (8). The cycles that emerge will be in the respective resistance and infection ranges of hosts and parasites, as demonstrated previously [4,27]. Figure 2b shows the output from simulations of the coevolutionary dynamics, once again showing regular cycles.

Assuming costs in the matching model (9) we again find that a Hopf bifurcation may always occur. However, in this case numerical analysis of the system indicated that the Hopf bifurcation is always *subcritical*, meaning that the cycles are unstable (i.e. not attracting) [35,36]. We explored a comprehensive range of parameter sets and trade-offs but saw no examples of stable coevolutionary cycles in bifurcation diagrams or numerical simulations. Instead there is generally a bistability such that, under the full assumptions of adaptive dynamics, the system should evolve either to an intermediate singular point or to a minimum. However, as is the case when there were no costs, when the assumptions are relaxed in numerical simulations we typically see fluctuating

317 selection. An example of these dynamics are shown in figure 2c where we see
318 rather irregular oscillations. These are once more non-deterministic, stochastic
319 oscillations. Such stochastic effects are inherent in natural systems and therefore
320 these oscillations are likely to occur in nature, but we emphasize that these are
321 less regular and predictable than those seen for the universal and range models
322 (c.f. figures 2a,b). Why do such oscillations emerge? In general the host will
323 always evolve away from the parasite and the parasite will evolve to match the
324 host, leading to a 'chase' across phenotypic space (which is again linked to the
325 presence of the 'trail' of strains present when mutations are not strictly rare).
326 However, we found that provided the trade-offs are not too strongly decelerating
327 or accelerating, the *h* and *p* nullclines generally remain very close to the main
328 diagonal (*h*=*p*) meaning that a small mutation can easily cross the nullclines and
329 reverse the direction of selection, causing the 'chase' to go in the other direction
330 (see figure S6 in the SI). These repeated crossings of the nullcline by small, finite
331 mutations are what drive the oscillations.
332
333 ***Host and parasite life-history characteristics***
334 We now explicitly consider the ecological conditions that favour FSD by varying
335 host and parasite life-history traits for each infection function. For the stable
336 cycles we do this by computing bifurcation diagrams using the numerical
337 continuation software AUTO-07p [37]. For the stochastic oscillations we examine
338 numerical simulations. In each case we shall explore the effects of altering (a)
339 resource competition, *q*, and (b) the virulence, . Plots for the other parameters
340 (*b*, and *f)* can be found in figures S2, S3 and S5 in the SI.
341

342 The behavior in the universal model as resource competition, *q,* is varied is
343 representative of all of the bifurcation diagrams (figure 3a, S2). The red vertical
344 dashed lines in figure 3 separate the regions of behavior, as annotated along the
345 bottom. Starting from the right-hand end of figure 3a, the trend as *q* is decreased
346 is: no singular point, leading to minimization; the emergence of a pair of singular
347 points through a saddle-node bifurcation (solid line: a branching point, dashed
348 line: a repeller) often leading to branching; a Hopf bifurcation leading to the
349 onset of cycles which increase in size (solid grey line marks the maximum and
350 minimum values reached on a cycle); the loss of cycles such that both host and
351 parasite maximize (i.e. ARD). We see similar behavior in figure 3b as virulence is
352 varied (although here the saddle-node bifurcation occurs for rates of virulence
353 beyond the domain of this plot). Decreasing values of *q* and *α* lead to increased
354 densities of infectious individuals, and hence higher encounter rates with
355 susceptible hosts. It is interesting to note that "static diversity" (branching to
356 coexistence) occurs for lower encounter rates than "temporal diversity" (FSD).
357 We conclude that FSD will be promoted in intermediate/large sized populations
358 (intermediate *q*, low *b*, intermediate *f*) with an intermediate infectious period
359 (intermediate , low *b*, intermediate). In §A3 and figure S5 in the SI we also
360 show that cycles occur for a range of weakly decelerating trade-offs in both the
361 host and parasite.
362
363 The bifurcation plots for the range model in figures 3c,d show very similar
364 behavior to those for the universal model (figures 3a,b), except that a new
365 behavior emerges with regions where the singular point is an attracting

366 *Continuously Stable Strategy* (CSS). The conditions that promote FSD in the range
367 model are qualitatively similar to those in the universal model.
368
369 To explore the effects of life-history characteristics on the stochastic oscillations
370 in the matching model we ran evolutionary simulations and measured the
371 variance in the host trait over the final 20% of each run. A higher variance
372 indicates larger stochastic oscillations (the values where there is zero variance
373 actually relate to parasite extinction). In figure 4 (figure S3 in the SI) we see a
374 similar pattern to the above results – the variance is greatest in long-lived (low
375 b), large populations (low q, low b) with high infectious periods
376 (low α, low γ, low b).
377
378
379 **Discussion**
380
381 We have analyzed a series of host-parasite coevolutionary models to understand
382 how ecological dynamics, life-history characteristics, and the specificity of
383 interactions between hosts and parasites impact fluctuating selection dynamics
384 (FSD). A key finding is that FSD in host resistance and parasite infectivity may
385 occur without the need for any specificity in the interaction between hosts and
386 parasites. When there is specificity, we find that the nature of fluctuating
387 selection is very different in a highly specific matching interaction (akin to
388 matching alleles in that all parasite strains are specialists on respective host
389 strains) compared to when there is variation in the range of specificity (akin to
390 gene-for-gene in that there is variation in specificity such that hosts and

391 parasites vary from specialists to generalists). Therefore, although it is already
392 known that both types of specific infection mechanism can lead to FSD, our
393 models suggest that the nature of the underlying fluctuations are fundamentally
394 different [see also 9]. Finally, we show how both host and parasite
395 characteristics influence the likelihood of fluctuating selection, which allows us
396 to predict the ecological conditions that are most likely to show FSD. This is
397 important because it tells us when fluctuating selection is likely to generate
398 genetic diversity through time [13].
399
400 The fact that fluctuating selection can arise without specificity between hosts
401 and parasites is of particular interest because much theoretical and empirical
402 work has focused on identifying the relationship between different types of
403 specificity and FSD rather than considering the potential for FSD in non-specific
404 interactions [7-11; 23-25]. We have shown that costs associated with non-
405 specific resistance and infectivity can be sufficient to generate coevolutionary
406 cycles in an eco-evolutionary setting. In principle, these cycles would also be
407 possible in a non-ecological framework where selection is frequency-dependent
408 but not density-dependent, as one could choose fitness functions whereby the
409 selection gradients are never simultaneously zero on a closed trajectory.
410 However, it is realistic to assume that the relative population densities, and thus
411 the prevalence of infection, will vary with changes in host resistance and parasite
412 infectivity. The feedbacks generated by these changes provide a natural route for
413 frequency-dependent selection to operate and generate fluctuations. The drivers
414 of the cycles in both the universal and range models are thus due to a mix of
415 frequency-dependence (i.e. relative infection rates) and density-dependence (i.e.

varying population sizes due to ecological feedbacks). Cycles without specificity have not been described previously, as most studies on FSD have neglected ecological dynamics and feedbacks. Those evolutionary studies that do include ecology have either assumed specificity between host and parasite and not examined universal interactions [16, 38-44], or, have assumed universal infection but focused on optimal investment or evolutionary branching rather than cycling [1-5; 29]. Our work examines models with explicit ecological dynamics and focuses on the potential for FSD both with and without specificity.

Ecology has been shown to drive fluctuating selection in predator-prey systems with specificity [31,45] (although we note that the `matching' function considered in these studies is different from the one used here). However, our work shows that it also occurs in non-specific host-parasite interactions. This result has important relevance to the role host-parasite coevolution may play in shaping host diversity across space and time. When host fitness depends on the frequency of different parasite genotypes, there are predicted to be differences among populations in terms of which host and parasite genotypes are being selected for at a given point in time. Hence, the propensity for fluctuating selection will have impacts on host–parasite local adaptation, as isolated populations are likely to be out of sync with one another [19,46]. There are also implications to the theory surrounding the evolution of sexual reproduction. While evolution of sex studies typically take a population genetics approach with a few major loci, it has been shown that sex can be beneficial where there are many loci with small additive effects [47]. One common criticism of the Red Queen hypothesis for the maintenance of sex is the lack of highly specific and

441 virulent parasites that are generally assumed to be necessary for FSD [48]. Our
442 work suggests these restrictive assumptions could be relaxed; future theory
443 must test whether selection for sex can be generated in the absence of specificity
444 and for parasites with only intermediate levels of virulence.
445
446 While we found that FSD could occur across all of the interactions we considered,
447 we found that the nature of the cycles are fundamentally different. We have
448 shown that both the universal and range infection functions can lead to regular,
449 deterministic cycles when there are costs. For the universal function this leads to
450 fluctuations in the transmission rate, while for the range function the
451 fluctuations are between pure generalists and pure specialists. However, when
452 there is a matching function we found that stable deterministic cycles do not
453 exist. Instead we have shown that oscillations occur driven by the inherent
454 incompatibility of the optimal host and parasite strategies. This result is in
455 accordance with models of matching alleles in continuous time, which have
456 shown only damped cycles rather than deterministic stable limit cycles [43,49].
457 This result also relates to the idea of 'stochastic persistence' [50], since regular
458 input of mutations (i.e. faster than a full separation of ecological and
459 evolutionary timescales) is essential for the cycles to be sustained. There are a
460 number of implications to these different types of cycles. The deterministic
461 cycles generated by the universal and range models are more regular and
462 consistent, making their behavior more predictable. In contrast, the stochastic
463 oscillations of the matching interaction tend to be irregular and vary in period
464 and amplitude, making their behavior unpredictable. Stochastic fluctuations may
465 also be less robust to changes in assumptions about mutation and standing

466 variation. Distinguishing between these two forms of cycles empirically would be
467 challenging due to environmental variation, but if FSD can be observed over
468 multiple cycles, evidence of regularity could be looked for. An exciting question
469 that thus emerges is whether the inherent differences among the fluctuating
470 dynamics observed across infection interactions might support different levels of
471 genetic diversity within and among populations. It is yet unclear whether cycles
472 generated under a specialist-generalist continuum (i.e. range or gene-for-gene)
473 framework can be considered equivalent to those generated under a purely
474 specialist (i.e. matching) framework.
475
476 By including explicit ecological dynamics in our models we have been able to
477 assess how host and parasite life-history characteristics impact the potential for
478 FSD. We have found that, no matter the infection function, cycles are most likely
479 when hosts are long-lived and exist at high, but not the highest, densities. These
480 results suggest that cycles are promoted when encounter rates are reasonably
481 high. When encounter rates are low, so too is the potential for infection;
482 therefore selection for costly host resistance is likely to be limited. At the other
483 extreme, if encounter rates are very high then there will be considerable
484 selection for resistance leading to an 'arms race dynamic' (ARD). It is in between
485 these two extremes when cycles are most likely to occur. These results
486 emphasise the role ecology plays in driving FSD in our models, since cycles only
487 arise for certain regions of parameter space. Empirical studies in bacteria-phage
488 systems agree with the predictions from our models, with environmental
489 conditions that increase host-parasite encounter rates causing a shift from FSD
490 to ARD [26-28]. This pattern is consistently seen in the stochastic oscillations

491 from the matching model as well as the stable cycles of the universal and range
492 models, suggesting this parameter dependency is robust.
493
494 Our models have demonstrated that there are a wide range of interactions
495 between hosts and parasites that can lead to fluctuating selection. We require
496 that there are costs to resistance and infectivity to produce deterministic cycles
497 in range or universal models, consistent with previous theory showing that costs
498 are necessary but not sufficient for FSD to occur in gene-for-gene systems [3].
499 However, highly specific matching interactions produce stochastic oscillations.
500 Our models are novel in that they demonstrate that specificity is not required for
501 fluctuating selection to occur. Both the host life-history and the disease
502 characteristics that promote FSD are consistent across all the different infection
503 interactions. We can therefore make robust predictions for the types of host-
504 parasite interactions that are most likely to lead to coevolutionary cycles. We
505 note that the timescale of the cycles seen in our models is somewhat slower than
506 those seen in classic gene-for-gene or matching-allele models. This is because we
507 assume a separation of ecological and evolutionary timescales, whereas the
508 genetic models are essentially at an ecological timescale with multiple competing
509 strains. The cycles considered here are purely at the evolutionary timescale, with
510 the population dynamics always being at, or close to (in simulations), an
511 equilibrium. We also note that our methods assume a large number of loci with
512 small additive effects, as opposed to classic population genetics models, which
513 generally assume a small number of loci and epistasis between them. Future
514 work will address when the discreteness that arises from a smaller number of
515 loci has a significant effect on the results, but without a detailed understanding of

the genetic basis of a particular interaction the quantitative assumption gives general insights.

Empirical evidence from a number of host-parasite systems indicates that fluctuating selection is a common form of coevolutionary dynamics. Several studies have reported indirect evidence of FSD (or host-parasite relationships capable of FSD) based on phylogenetic data (e.g. *Arabidopsis* plants and *Pseudomonas* bacteria [51]), highly specific genetic interactions (e.g. sticklebacks and trematodes [52]), or high levels of polymorphism in immune genes (e.g. in the vertebrate Major Histocompatibility Complex [53]). Direct evidence of FSD primarily comes from time-shift experiments [54] between crustaceans and bacteria [55], water snails and trematodes [56], and bacteria and phages [26-28; 57]. The predictions from our models therefore have wide relevance within coevolutionary host-parasite systems. Given the ubiquity of ecological feedbacks and the diversity of different infection interactions our work emphasizes the considerable potential for host-parasite coevolution to generate fluctuating selection.

Author Contributions

ABe conceived of and designed the study, carried out the mathematical modeling and simulations, and drafted the manuscript. BA carried out mathematical modeling and simulations, and helped draft the manuscript. AW helped design the study and helped draft the manuscript. RB helped carry out the mathematical modelling and helped draft the manuscript. ABu helped design the study and

helped draft the manuscript. BK helped design the study and helped draft the manuscript. MB conceived of and designed the study and drafted the manuscript.

Acknowledgements

We thank two anonymous reviewers for their comments on an earlier version of this manuscript.

Ethics

No ethics approval was needed for this study.

Funding

Alex Best was funded by a Leverhulme Early Career Fellowship, and this work was supported by NERC grants NE/J009784/1 and NE/N014979/1.

Data Accessibility

No data is used in this study. C++ code used for the simulations can be found in the supplementary material.

Competing Interests

We have no competing interests.

References

1. van Baalen, M. (1998). Coevolution of recovery ability and virulence. *Proc R. Soc. B.*, 265(1393):317–325.
2. Best, A., White, A. and Boots, M.. (2009). The Implications of Coevolutionary Dynamics to Host-Parasite Interactions. *American Naturalist* 173:779-791.
3. Tellier, A. and J. K. M. Brown (2007). Stability of genetic polymorphism in host-parasite interactions. *Proc R. Soc. B.*, 274:809–817.
4. Best, A., A. White, E. Kisdi, J. Antonovics, M. A. Brockhurst, and M. Boots. (2010). The Evolution of Host-Parasite Range. *American Naturalist* 176:63-71.
5. M. Boots, A. White, A. Best, and R. G. Bowers (2014). How specificity and epidemiology drive the coevolution of static trait diversity in hosts and parasites. *Evolution*, 68:1594-1606.
6. Gandon, S., Buckling, A., Decaestecker, E. and Day, T. (2008). Host-parasite coevolution and patterns of adaptation across time and space. *J. Evol. Biol.*, 21:1861-1866.
7. Flor, H.H. (1956). The complementary genetic systems in flax and flax rust. *Adv. Genet.*, 8:29-54.
8. Jayakar, S. (1970). A mathematical model for interaction of gene frequencies in a parasite and its host. *Theor Pop Biol.*, 1:140-164.
9. Sasaki, A. (2000). Host-parasite coevolution in a multilocus gene-for-gene system. *Proc R. Soc. B.* 267:2183-2188.

584 10. Agrawal, A. and C. M. Lively. (2002). Infection genetics: gene-for-gene
585 versus matching-alleles models and all points in between. *Evolutionary*
586 *Ecology Research* 4:79-90.
587 11. Ashby, B. and Boots, M. (2017). Multi-mode fluctuating selection in host-
588 parasite coevolution. *Ecology Letters*, 20:357-365.
589 12. Hall, A., Scanlan, P., Morgan, A. and Buckling, A. (2011). Host-parasite
590 coevolutionary arms races give way to fluctuating selection. *Ecology*
591 *Letters*, 14:635-642.
592 13. Clarke, B. (1979). Evolution of genetic diversity. *Proc Roy Soc. B.*, 205:453-
593 474.
594 14. Hamilton, W. D. (1980). Sex versus non-sex versus parasite. *Oikos*, 35:
595 282-290.
596 15. Lively, C. (2009). The maintenance of sex: host-parasite coevolution with
597 density-dependent virulence. *J. Evol. Biol.*, 22:2086-2093.
598 16. Lively, C. (2010). An epidemiological model of host-parasite coevolution
599 and sex. *J. Evol. Biol.*, 23:1490-1497.
600 17. Lively, C. (1999). Migration, virulence and the geographic mosaic of
601 adaptation by parasites. *Am. Nat.*, 153:S34-S47.
602 18. Gandon, S. (2002). Local adaptation and the geometry of host-parasite
603 coevolution. *Ecology Letters*, 5: 246-256.
604 19. Morgan, A., Gandon, S. and Buckling, A. (2005). The effect of migration on
605 local adaptation in a coevolving host-parasite system. *Nature*, 437:253-
606 256.
607 20. Frank, S. A. (1993). Coevolutionary genetics of plants and pathogens. *Evol.*
608 *Ecol.* 7:45-75.

609 21. S. A. Frank (1994). Coevolutionary genetics of hosts and parasites with
610 quantitative inheritance. *Evol. Ecol*. 8:74–94.
611 22. Hamilton, WD (1993). Haploid dynamic polymorphism in a host with
612 matching parasites – effects of mutation subdivision, linkage and patterns
613 of selection. *J. Heredity*, 84:328-338.
614 23. Thrall, P and Burdon, J. (2003). Evolution of virulence in a plant host-
615 pathogen metapopulation. *Science*, 299:1735-1737.
616 24. Scanlan, P., Hall, A., Lopez-Pascua, L, et al. (2011). Genetic basis of
617 infectivity evolution in bacteriophage. *Mol. Ecol.*, 20:981-989.
618 25. Luijckx, P., Fienberg, H., Duneau, D. et al. (2013). A matching allele model
619 explains host resistance to parasites. *Curr. Biol.,* 23:1085-1088.
620 26. Gomez, P. and A. Buckling (2011). Bacteria-phage antgaonistic
621 coevolution in soil. *Science*, 332:106–109.
622 27. Lopez-Pascua, L., A. Hall, A. Best, A. D. Morgan, M. Boots, and A. Buckling
623 (2014). Higher resources decrease fluctuating selection during host-
624 parasite coevolution. *Ecology Letters*, 17:1380–1388.
625 28. Gomez, P., Ashby, B. and Buckling, A. (2015). Population mixing promotes
626 arms race host-parasite coevolution. *Proc. Roy. Soc. B.*, 282:20142297.
627 29. Gandon, S., P. Agnew, and Y. Michalakis (2002). Coevolution between
628 parasite virulence and host life-history traits. *American Naturalist*,
629 160(3):374–388.
630 30. Dieckmann, U. and R. Law (1996). The dynamical theory of coevolution: a
631 derivation from stochastic ecological processes. *Journal of Mathematical*
632 *Biology*, 34(5-6):579–612.

633 31. Marrow, P., U. Dieckmann, and R. Law (1996). Evolutionary dynamics of
634 predator-prey systems: an ecological perspective. *Journal of Mathematical*
635 *Biology*, 34:556–578.
636 32. Metz, J.A.J., S. A. H. Geritz, G. Mesz ena, F. J. A. Jacobs, and J. S. Van
637 Heerwaarden (1996). Adaptive dynamics: a geometrical study of the
638 consequences of nearly faithful reproduction. In S. J. van Strein and S. M.
639 Verduyn Lunel, editors, *Stochastic and Spatial Structures of Dynamical*
640 *Systems*, pages 183– 231. Elsevier: North-Holland.
641 33. Geritz, S. A. H., E. Kisdi, G. Meszena, and J. A. J. Metz. (1998). Evolutionarily
642 singular strategies and the adaptive growth and branching of the
643 evolutionary tree. *Evolutionary Ecology* 12:35-57.
644 34. Anderson, R. M. and R. M. May (1979). Population biology of infectious
645 diseases: Part I. *Nature*, 280:361–367.
646 35. Kuznetsov, Y.. *Elements of Applied Bifurcation Theory*. Springer, 1995.
647 36. Kisdi E., Geritz, S. and Boldin, B. (2013). Evolution of pathogen virulence
648 under selective predation: a construction method to fins eco-evolutionary
649 cycles. *J. Theor. Biol.* 339:140-150.
650 37. Doedel, E. J. and B. E. Oldeman. *AUTO-07P: Continuation and bifurcation*
651 *software for ordinary differential equations*. Technical report, Concordia
652 University, Montreal, Canada, 2009.
653 38. May, R. M. and Anderson, R. M. (1983). Epidemiology and genetics in the
654 coevolution of parasites and hosts. *Proc. R. Soc. B.*, 219:281-313.
655 39. Tellier, A. and Brown, J. (2008). The relationship of host-mediated
656 induced resistance to polymorphism in gene-for-gene relationships.
657 *Phytopathology*, 98:128-136.

40. Gandon, S. and Day, T. (2009). Evolutionary epidemiology and the dynamics of adaptation. *Evolution*, 826-838.
41. Quigley, B. Z., Garcia Lopez, D., Buckling, A. *et al.* (2012). The mode of host-parasite interaction shapes coevolutionary dynamics and the fate of host cooperation. *Proc R. Soc. B.,* 279:3742-3748.
42. Gokhale, C., Papkou, A., Traulsen, A. and Schulenburg, H. (2013). Lotka–Volterra dynamics kills the Red Queen: population size fluctuations and associated stochasticity dramatically change host-parasite coevolution. *BMC Evol. Biol.*, 13:254.
43. Ashby, B. and Gupta, S. (2014). Parasitic castration promotes coevolutionary cycling but also imposes a cost on sex. *Evolution*, 68:2234-2244.
44. Ashby, B., Gupta, S. and Buckling, A. (2014). Effects of epistasis on infectivity range during host-parasite coevolution. *Evolution*, 68:2972-2982.
45. Marrow, P., R. Law, and C. Cannings. (1992). The coevolution of predator-prey interactions: ESSs and Red Queen dynamics. *Proc R. Soc. B.*, 250:133–141.
46. Gandon, S., Buckling, A., Decaestecker, E. and Day, T. (2008). Host-parasite coevolution and patterns of adaptation across time and space. *J. Evol. Biol.*, 21:1861-1866.
47. Doebeli, M. (1996). Quantitative genetics and population dynamics. *Evolution*, 50:532-546.
48. Otto, S. and Nuismer, S. (2004). Species interactions and the evolution of sex. *Science*, 304:1018-1020.

683 **49.** Kouyos, R., Aslathe, M. and Bonhoeffer, S. (2007). The Red Queen and the
684 persistence of linkage-disequilibrium oscillations in finite and infinite
685 populations. *BMC Evol. Biol.*, 7:211.
686 50. Allen, J. (1975). Mathematical models of species interactions in time and
687 space. *Am. Nat.*, 967:319-342.
688 51. Stahl, E., Dwyer, G., Mauricio, R. et al. (1999). Dynamics of disease
689 resistance polymorphism at the Rpm1 locus of Arabidopsis. *Nature*,
690 400:667-671.
691 52. Rauch, G., Kalbe, M., and Reusch, T. (2006). One day is enough: rapid and
692 specific host-parasite interactions in a stickleback-trematode system.
693 *Biology Letters*, 2:382-384.
694 53. Penman, B., Ashby, B. Buckee, C. et al. (2013). Pathogen selection drives
695 nonoverlapping associations between HLA loci. *Proc Nat. Acad. Sci.*,
696 110:19645-19650.
697 54. Gaba, S. and Ebert, D. (2009). Time-shift experiments as a tool to study
698 antagonistic evolution. *Trends in Ecol. Evol.*, 24:226-232.
699 55. Decaestecker, E., Gaba, S., Raeymaekers, J. et al. (2007). Host-parasite 'Red
700 Queen' dynamics archived in pond sediment. *Nature*, 450:870-U16.
701 56. Koskella, B. and Lively, C. (2007). Advice of the rose: experimental
702 coevolution of a trematode parasite and its snail host. *Evolution*, 61:152-
703 159.
704 57. Koskella, B. (2014). Bacteria-phage interactions across time and space:
705 merging local adaptation and time-shift experiments to understand phage
706 evolution. *Am Nat*, 184:S9-S21
707

Figure Legends

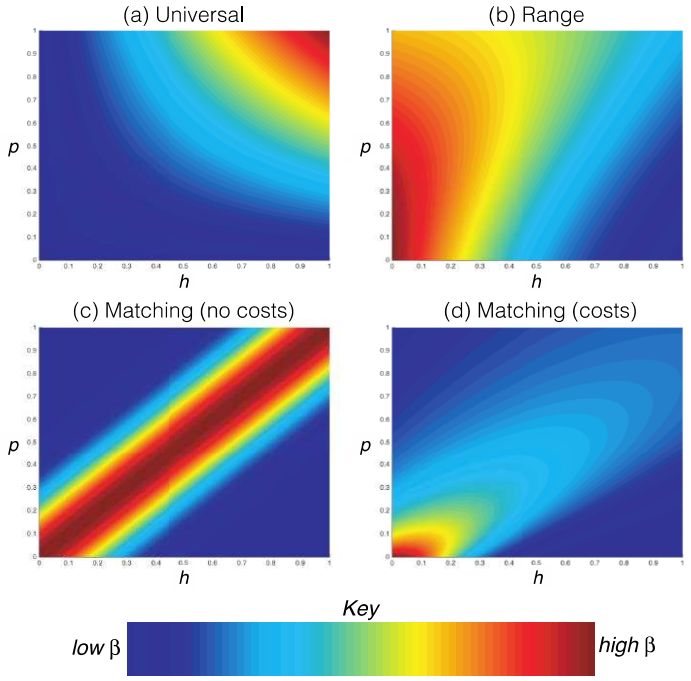

Figure 1

Heat maps showing the level of transmission, β, of parasite strains, p, against host strains, h, for our key infection functions: (a) Universal, (b) Range, (c) Matching without costs and (d) Matching with costs. The key shows that red indicates the highest transmission and blue the lowest transmission. Horizontal slices through these plots, showing β as a function of h for particular values of p, can be found in figure S1 in the SI. The exact forms are: (a) $\beta(h,p) = hp + 0.5$, (b) $\beta(h,p) = \beta_0(p)(1 - 1/(1 + \exp(3(p-h)))$ with $\beta_0(p) = 0.3 + 0.5(1 - p)/(1 + 1.45p)$, (c) $\beta(h,p) = \exp(-(p-h)^2/0.25^2)$, (d) $\beta(h,p) = \beta_0(p)(\exp(-(p-h)^2/(0.8p + 0.25)^2)$ with $\beta_0(p) = 15 - 12p/(1 + 0.85(p-1))$. We note that the explicit form of our trade-offs link maximum and minimum trait values through a smooth, polynomial-like curve where the second-derivative has constant sign (i.e. no inflections).

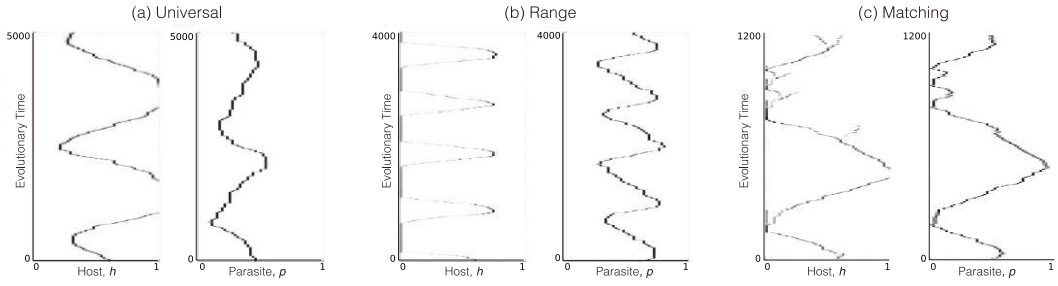

Figure 2

Output from numerical simulations showing the investment in host defence, h, and parasite infectivity, p, over evolutionary time using the three infections functions from figure 1: (a) Universal, (b) Range, (c) Matching. Simulations were conducted as described in the SI. In (a) $q = 0.1, b = 1, f = 0, \alpha_c = 5, \gamma = 0.1$, in (b) $q = 0.2, b = 1, f = 0, \alpha = 9, \gamma = 0.001$ and in (c) $q = 0.1, b = 1, f = 0, \alpha = 9$ $\gamma = 0.1$. The parasite trade-off in (a) is $\alpha(p) = \alpha_c + 0.67 + 6.67p/(1 - 0.001(1 - p))$ and in (b) and (c) as given in figure 1. The host trade-offs are (a) $a(h) = 7.77 + 4.51h/(1 + 0.04(1 - h))$, (b) $a(h) = 55 + 45(1 - h)/(1 + 0.13h)$, (c) $a(h) = 30 - 20h/(1 + 0.2(h - 1))$. We note that these trade-offs are not subject to the assumptions made when proving the existence of the Hopf bifurcation in the SI (indeed if we chose trade-offs that satisfied those conditions, we would not see cycles in the simulations).

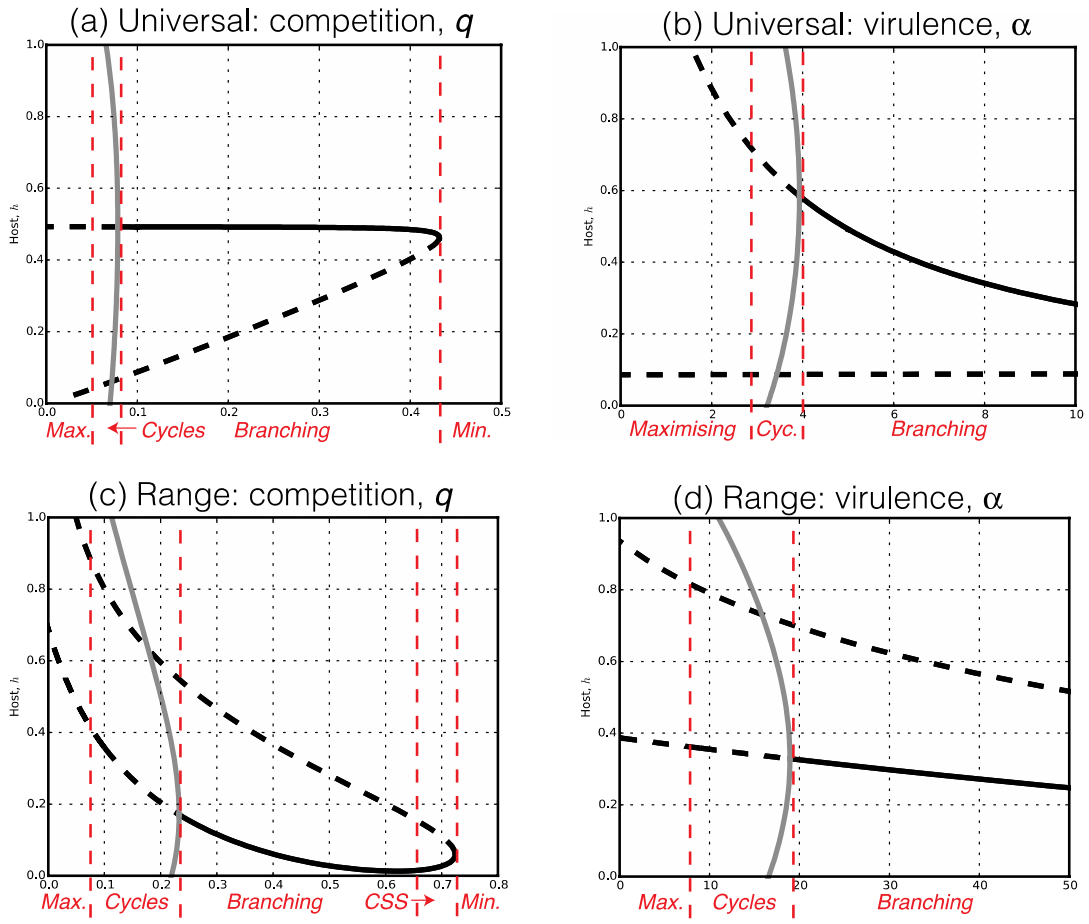

Figure 3

Bifurcation diagrams for (top row) the universal and (bottom row) range models showing the change in behavior at the singular point as we vary: (a), (c) competition, q, and (b), (d) virulence, α, in terms of host investment, h. Solid black lines denote convergence stable singular points, dashed black lines non-convergence stable singular points (i.e. repellers) and solid gray lines the upper and lower limits of a coevolutionary cycle. The red vertical dashed lines separate regions of behavior as annotated along the bottom of the plots. The *Maximize* and *Minimize* labels refer to the host's behaviour. In these regions the parasite either displays the same behavior or reaches a CSS. Default parameter values are: $q = 0.1, b = 1, f = 0$ with (a) and (b) $\alpha_c = 5, \gamma = 0.1$, and (c) and (d) $\alpha = 9, \gamma = 0.001$ with the trade-offs as given in figures 1 and 2. Again, we note that these

752 trade-offs are not subject to the assumptions made when proving the existence
753 of the Hopf bifurcation
754
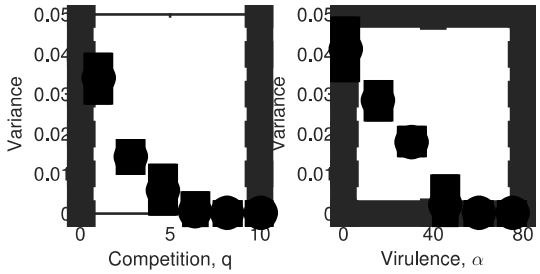

755
756 **Figure 4**
757 Plots showing the variance in the host trait over the final 20% of numerical
758 simulations, using the matching model for (a) competition, *q,* and (b) virulence,
759 α. A larger variance indicates larger cycles. Zero variance occurs where there is
760 parasite extinction. Parameter values are as of figure 2.
761